THE JOURNAL OF PHYSICAL CHEMISTRY C

Subscriber access provided by UNIV NAC DE LA PLATA

Article

Electrochemical and X-ray Photoelectron Spectroscopy Characterization of Alkanethiols Adsorbed on Palladium Surfaces

Gasto#n Corthey, Aldo A. Rubert, Guillermo A. Benitez, Mariano H. Fonticelli, and Roberto C. Salvarezza

J. Phys. Chem. C, **2009**, 113 (16), 6735-6742• DOI: 10.1021/jp9001077 • Publication Date (Web): 26 March 2009

Downloaded from http://pubs.acs.org on April 25, 2009

More About This Article

Additional resources and features associated with this article are available within the HTML version:

- Supporting Information
- Access to high resolution figures
- Links to articles and content related to this article
- Copyright permission to reproduce figures and/or text from this article

View the Full Text HTML

ACS Publications
High quality. High impact.

The Journal of Physical Chemistry C is published by the American Chemical Society. 1155 Sixteenth Street N.W., Washington, DC 20036

Electrochemical and X-ray Photoelectron Spectroscopy Characterization of Alkanethiols Adsorbed on Palladium Surfaces

Gastón Corthey, Aldo A. Rubert, Guillermo A. Benitez, Mariano H. Fonticelli,* and Roberto C. Salvarezza

Instituto de Investigaciones Fisicoquímicas, Teóricas y Aplicadas (INIFTA), Universidad Nacional de La Plata - CONICET, Sucursal 4 Casilla de Correo 16 (1900) La Plata, Argentina

Received: January 6, 2009; Revised Manuscript Received: February 27, 2009

The self-assembly of alkanethiolate monolayers on palladium substrates and their stability in aqueous solutions have been studied by electrochemical techniques and X-ray photoelectron spectroscopy (XPS). Alkanethiols adsorb on Pd from ethanolic solutions forming a complex interface which consists of thiolates onto a diluted palladium sulfide interphase, with surface coverages $\theta_{\text{Sulfide}} \approx 0.4$ and $\theta_{\text{thiolate}} \approx 0.30$, respectively. These complex adlayers exhibit hydrocarbon chain-length dependent barrier properties like those formed on Au and Ag substrates. For short chain alkanethiols, thiolates are more stable against reductive desorption than self-assembled monolayers (SAMs) on Au, Ag, and Ni. The increased stability of the organic species seems to be related to the presence of the diluted sulfide layer that also explains the chain length independence of the stability potential range. The stability of these monolayers in aqueous solutions indicates that Pd is a suitable platform for thiolate-based devices such as sensors and biosensors. These results also suggest that electrochemical cleaning should be a simple way to prepare metallic nanoparticles from thiol-capped Pd nanoparticles adsorbed on conducting substrates.

1. Introduction

The preparation and characterization of alkanethiolate self-assembled monolayers (SAMs) on metals has attracted considerable attention because of the possibility to control the order and interactions of different systems at the molecular level.[1] This has triggered several innovative applications, ranging from molecular electronics to biosensors.[1,2] Most of the experimental and theoretical work has been done using Au, Ag, and Cu as substrates.[3−6] In contrast, the knowledge of the formation, physicochemical properties, and stability of SAMs on Pt and Pd surfaces is relatively scarce.[7−11] The alkanethiol−Pd system is particularly interesting because the organic molecules/metal interface seems to involve a mixed layer containing sulfide and alkanethiolate species.[7] The palladium-sulfide interphase, which has been proposed based on X-ray photoelectron spectroscopy (XPS) measurements,[7] enhances the SAM stability against the wet-chemical etchants, compared with the alkanethiolate SAMs on Au.[12] Although thiols are usually used as a protecting cap for Pd nanoparticles,[13] massive sulfidization of alkanethiol-capped Pd nanoparticles has been reported.[14−16] Both in planar and curved Pd surfaces, the S atoms could be formed due to the S−C bond scission during alkanethiol self-assembly or cluster growth, respectively.[7,14] Furthermore, many catalytic processes were limited by Pd sulfidization or by the action of alkanethiol moieties. Alkanethiol-protected Pd nanoparticles have been used as hydrogen sensors because of the ability of Pd to absorb large amounts of this element.[17] It was found that the capping agent acts as a blocking layer hindering hydrogen absorption. For this reason, it is necessary the cleaning of the nanoparticle surface prior to its use as a sensor. On the other hand, aromatic thiols protect the Pd catalyst against deactivation during the oxidation of formic acid.[18] With regards to the exceptional properties of alkanethiol monolayers on Pd, it has been shown that they are superior to monolayers on gold and silver for patterning microstructures by microcontact printing.[12] In a replacement lithography study using a scanning tunneling microscopy (STM) tip on alkanethiol monolayers on Au(111), Pd(111), and Pt(111), it was found that replacement correlates well with metal work function. This suggests that desorption depends on the metal's ability to introduce electrons into the thiol moiety.[19] However, the alkanethiolate monolayers structure on Pd and its electrodesorption are far from being understood. In fact, a recent first-principles study on the adsorption behavior of thiols on Pd(111)[20] does not take into account the sulfur interlayer mentioned above.[7]

In the field of electrochemistry, alkanethiol monolayers have been prepared onto electrodeposited Pd multilayers.[9] Nevertheless, no information about the Pd-thiol interface structure or its electrochemical stability was reported. More recently, the reductive desorption of alkanethiols from the Pd surface has been studied.[21] In contrast to Au[22] and Ag,[23,24] no electrodesorption peak was observed despite the fact that the organic layer could be desorbed from Pd surfaces at potentials which are similar to those reported for Au surfaces, as detected by the redox couples behavior in solution. Surprisingly, no dependence of the reductive desorption potential range on the hydrocarbon chain length was found. The complexity of the sulfide-thiolate adlayer and the anomalous behavior of its reductive desorption make this system particularly attractive for basic research.

In this work, we have studied the barrier properties and the electrochemical stability of alkanethiolate-sulfide adlayers on Pd surfaces against reductive desorption by using XPS and electrochemical techniques. The adlayers have been prepared in liquid phase by immersion of the substrate in alkanethiol-containing ethanolic solutions. XPS and electrochemical data confirm the presence of a complex layer formed by palladium

* Corresponding author. Fax: (+54) 221425 4642. Phone: (+54) 221425 7430. E-mail: mfonti@inifta.unlp.edu.ar. Homepage: http//nano.quimica.unlp.edu.ar.

10.1021/jp9001077 CCC: $40.75 © 2009 American Chemical Society
Published on Web 03/26/2009

sulfide and terminated by the alkanethiolate SAM. Capacitance measurements and charge transfer to a redox couple show the presence of a dense organic barrier that hinders the hydrogen evolution reaction and H absorption/adsorption. Combined electrochemical and XPS data clearly show that in the aqueous alkaline media, reductive desorption takes places at more negative potential values than those found for a similar thiol on Au, Ag and Ni surfaces. The stability of the sulfide palladium layer toward reductive desorption seems to be responsible for the electrochemical stability of SAMs.

2. Experimental Methods

2.1. Electrochemical Experiments. Standard three-electrode electrochemical cells were employed with an operational amplifier potentiostat (TEQ-Argentina). A saturated calomel electrode (SCE) and a large-area platinum foil were used as reference and counter electrode, respectively. All potentials in the text are referred to the SCE scale. The base electrolyte, a 0.1 M NaOH aqueous solution, was prepared with Milli-Q water and solid NaOH (analytical grade from Baker) and was degassed with purified nitrogen prior to the experiments.

2.2. Preparation of the Substrates. Alkanethiols were adsorbed on Pd substrates prepared by Pd electrodeposition onto preferred oriented Au(111) substrates. These Au(111) substrates were obtained by annealing polycrystalline Au samples (Arrandee) with a hydrogen flame for 10 min. Atomically smooth (111) terraces separated by steps of mono or diatomic height are obtained by this method, as observed by STM.[25] An aqueous solution of 1 mM $PdCl_2$ + 2 mM HCl + 0.1 M H_2SO_4 was used as the plating bath.[26] Pd electrodeposition was made by applying a potential ramp at 1 $mV \cdot s^{-1}$ from 0.80 to 0.40 V and waiting 10 min at the negative potential limit (0.40 V), i.e., in the overpotential deposition region (OPD). The overall charge density deposited under these experimental conditions is equivalent to approximately 50 monolayers of Pd. Pd terraces with (111) preferred orientation were obtained[27] as confirmed by STM (see the Supporting Information). After electrodeposition, the substrates were rinsed, first with 0.1 M H_2SO_4, then with Milli-Q water, and finally dried under a nitrogen atmosphere. The cleanness of the Pd substrates was tested electrochemically and by XPS.

The determination of the real surface area (A) of Pd electrodes was made by estimating the charge involved in the electroreduction of 1 PdO monolayer from cyclic voltammograms recorded in 0.1 M NaOH (peak CI in Figure 1b)[28,29] (for details, see the Supporting Information). All electrochemical data refer to the real surface area.

2.3. Preparation of the Alkanethiolate- and Sulfur-Covered Surfaces. Alkanethiolate monolayers on Pd were prepared in liquid phase using alkanethiols with different chain lengths (n carbons): propanethiol (C3), hexanethiol (C6), nonanethiol (C9), and dodecanethiol (C12). All of them were from Fluka and were used without further purification. The thiolate monolayers were prepared by immersing the Pd substrates in 50 μM alkanethiol ethanolic solutions overnight. After the preparation, the samples were carefully cleaned in ethanol in order to remove physisorbed thiols, and then they were used for the electrochemical and XPS characterization. S-covered Pd surfaces were prepared by immersion of the substrates in 60 μM Na_2S (Aldrich) + 0.1 M NaOH aqueous solutions for 1 min. Under these conditions S coverage was approximately one monolayer (see below for details about XPS data related to these samples).

2.4. XPS. The samples were characterized by XPS using a Mg Kα source (XR50, Specs GmbH) and a hemispherical electron energy analyzer (PHOIBOS 100, Specs GmbH). A two-point calibration of the energy scale was performed using sputtered cleaned gold (Au 4f7/2, binding energy (BE) = 84.00 eV) and copper (Cu 2p3/2, BE = 933.67 eV) samples. For spectra deconvolution of the S 2p region, a Shirley type background was subtracted and a combination of Lorentianz and Gaussian functions was used. The full width at half-maximum (fwhm) was fixed at 1.1 eV and the spin−orbit doublet separation of S 2p signal was set to 1.2 eV. The BEs and peak areas were optimized to achieve the best adjustment.

Sulfur coverage was estimated by the measurement of the areas of Pd 3d and S 2p signals corrected by the relative sensitivity factor (RSF) of the elements. The Pd 3d signal was corrected by the attenuation length for 3d electrons in Pd to consider only the signal of the top Pd atomic monolayer. Therefore, sulfur coverage (θ_S) is the ratio of sulfur atoms to Pd atoms on the surface, taking into account every chemical form of sulfur, unless stated.

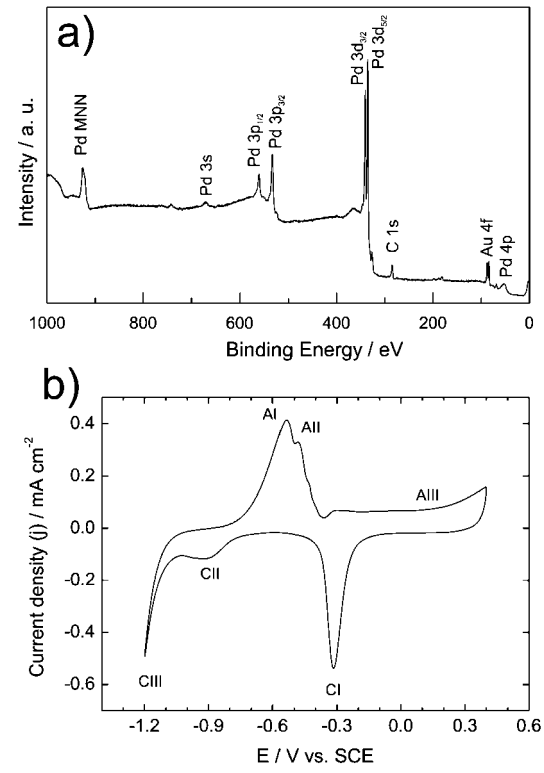

Figure 1. (a) XPS spectrum of electrodeposited Pd on Au. (b) Cyclic voltammogram of Pd (as-prepared) in NaOH 0.1 M. Scan rate: 100 $mV \cdot s^{-1}$.

3. Results and Discussion

3.1. XPS and Electrochemistry of Clean Pd. Typical XPS spectra obtained for electrodeposited Pd on Au used in our experiments is shown in Figure 1a. The absence of contaminants (Cl^-, S, and SO_4^{-2}) and oxidized Pd species is evident from the spectra. We have only observed a small amount of C resulting from atmospheric contaminants as a consequence of the transfer process.

Figure 1b shows a stationary voltammogram of Pd in 0.1 M NaOH which has been acquired after starting the potential scan at −0.4 V in the negative direction, until −1.2 V was reached, and repeatedly cycling the potential between −1.2 and +0.4 V. In the positive scan the Pd surface begins to be oxidized at 0 V and may be further oxidized at higher potentials. On the negative scan, the palladium oxide layer is reduced, showing a

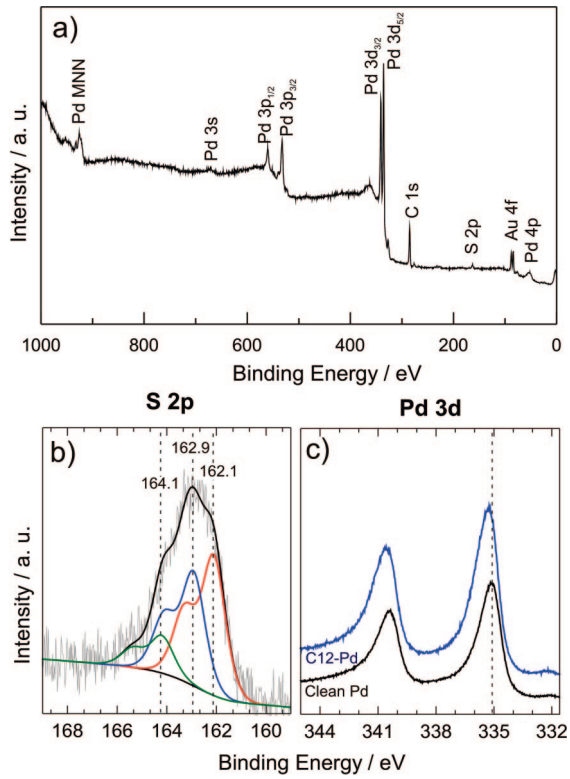

Figure 2. (a) XPS spectrum of a C12 SAM on Pd. (b) High-resolution XPS spectrum of the S 2p region. (c) High-resolution XPS spectrum of the Pd 3d region of a C12 SAM on Pd. Also the Pd 3d region of clean Pd is shown.

reduction peak at −0.35 V (CI). The small cathodic peak between −0.8 and −1.0 V (CII) is assigned to H adsorption reaction,[30] while the hydrogen evolution reaction (HER), which is overlapped with H absorption,[30,31] starts at −1.1 V (CIII). In the positive scan, the electrooxidation of the absorbed (AI) and adsorbed (AII) hydrogen originate broad and complex overlapped peaks around −0.6 V.[31]

Then, the freshly electrodeposited Pd surfaces, which were used to adsorb the different alkanethiol molecules from the ethanolic solutions, show reasonable level of contaminants. Particularly, they are free of sulfur species.

3.2. XPS of Alkanethiols Adsorbed on Pd. XPS data obtained after overnight incubation of clean Pd substrates in the C12 containing ethanolic solution are shown in Figure 2. We observe a broad S 2p signal typical of SAM-covered metals with three components at 162.1 eV, 162.9 and 164.1 eV (Figure 2b). The percentages of the different components and the corresponding assignments are shown in Table 1. The total S coverage (θ_S) obtained from the spectra was $\theta_S \approx 0.8$, a figure much larger than 0.33 and 0.44 reported for close packed alkanethiolate SAMs with molecules in vertical configuration formed on Au(111) and Ag(111), respectively.[3,23,32−35] The Pd signal, when compared to the clean Pd surface, exhibits a slight shift toward greater BE indicating partial Pd oxidation (Figure 2c). Although in these photoemission experiments there was not enough resolution to separate contributions from the bulk and surface atoms of the Pd system, the BE shift can be ascribed to the contribution of surface Pd atoms considering that sulfur coverage is within the submonolayer regime. We obtained similar results for the S 2p and Pd 3d signals for C3 on Pd, i.e. the nature of the S-metal interface is independent of the hydrocarbon chain length.

For C12 modified substrates, a strong C 1s signal was observed, which is consistent with the presence of the hydrocarbon chain (Figure 2a). This is not evident for the smaller C signal in the C3 covered Pd sample because of the presence of the small amount of C from atmospheric contaminants.

The large amount of S ($\theta_S \approx 0.8$), larger than expected for close packed thiolate monolayer, indicates that molecular species should coexist with a sulfur containing interlayer coming from the initial alkanethiol decomposition.[7] Therefore, we interpret our data following ref 7 for alkanethiol adlayers on Pd: adsorbed thiolates (162.9 eV component) are placed on sites of a diluted S layer (162.1 eV component) adsorbed on the substrate surface, a picture that is supported by the sulfide/thiolate ratio ≈ 1.2 derived from our spectra. This model is also supported by considering that S on Pd in ultrahigh vacuum environments forms interstitial surface phases.[36] The assignment of the small 164.1 eV component is more difficult and it could correspond to physisorbed disulfide molecules[7] or physisorbed alkanethiols.[37] However, samples exhaustively rinsed with ethanol and then measured again by XPS exhibit no changes in the intensity of the 164.1 eV signal. Therefore, it is possible to conclude that the 164.1 eV component is not associated with weakly adsorbed species as already concluded for alkanethiolates SAMs on Pt.[8] Then, the possibility of assigning the 164.1 eV to elemental S should not be disregarded considering that elemental S on metals are associated with higher BEs signals than those measured for sulfides or thiolates.[38] On the other hand, the 165 eV doublet in studies about alkanethiols on Pt was assigned to S^{4+} species.[8]

The XPS data allow us to conclude that the adsorption of alkanethiols on Pd leads to a complex adlayer consisting of thiolates and sulfides with a little amount of oxidized sulfur species.

3.3. Electrochemistry of Alkanethiolate-Sulfide Adlayers on Pd. The presence of a thiolate-containing adlayer at the Pd surface is reflected in the voltammogram (first cycle) recorded in 0.1 M NaOH (Figure 3). In fact, the double layer capacitance in the −1.20/−0.50 V potential range is much smaller than that for the clean Pd. The HER (CIII in Figure 3) is shifted in the negative direction indicating that the reaction is hindered. Accordingly, the oxidation of the absorbed hydrogen atoms is suppressed and the small peak related to H adsorption disappears. This means that the transport of water molecules is difficult through the hydrophobic hydrocarbon chains, so that there is a negligible population of adsorbed H which can diffuse into the Pd lattice (absorbed hydrogen). However, under repetitive scans the HER develops at a more positive potential and the current related to hydrogen electrooxidation (AI) starts to increase. This suggests that potential induced disorder or desorption of the thiolate monolayer takes place at the more negative potentials.

We have tested the barrier properties of our complex thiolate-sulfide adlayers on Pd by doing interfacial capacitance (C) measurements and studying the behavior of a redox couple in solution.

It is well-known that, when a long chain alkanethiol is used, the capacitances of alkanethiolate SAM covered electrodes in electrolyte solution are approximately 1 order of magnitude smaller than those of bare electrodes.[39] C is almost constant with potential and can be obtained by dividing the charging current density (j) by the scan rate (υ) in a potential range where no faradaic processes occur (oxidation or reduction reactions).[40−43] Although Pd electrochemistry in basic media is so complex and implies many oxidation and reduction processes (Figure 1b), it is possible to estimate the double layer capacitance by using cyclic voltammetry. We achieved that by scanning the electrode

TABLE 1: Assignment of the Different Components of the S 2p Signal of Alkanethiolate SAMs on Pd

alkanethiols adsorbed on Pd	assignment	sulphide	thiolate	−S−S− [b] or S, S^{+4c}
	BE[a,b](atomic %)	162.3 (44.4%)	163.2 (40.2%)	164.9 (15.4%)
	BE[a,c](atomic %)	162.1 ± 0.1 (48%)	162.9 ± 0.1 (39%)	164.1 ± 0.2 (13%)

sulfur adsorbed on Pd	assignment	PdS	PdS_2	S_n	oxidized S
	BE[a,d]	161.8	162.6	163.4	
	BE[a,c]	161.6 ± 0.1	162.4 ± 0.1	163.3 ± 0.1	165.2 ± 0.1

[a] eV. [b] Data taken from ref 7. [c] Data from this work. [d] Data taken from ref 53.

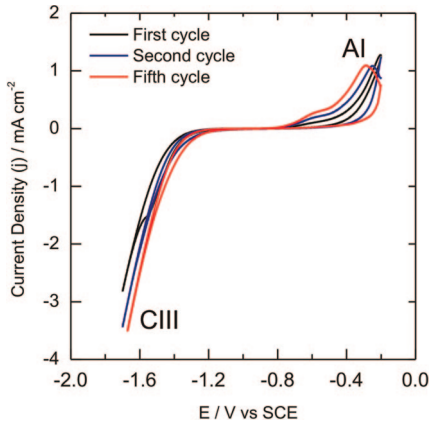

Figure 3. Cyclic voltammograms of a C12 covered Pd electrode. The potential was scanned between −0.20 and −1.70 V at 50 mV·s^{-1} in order to study de reductive electrodesorption processes.

TABLE 2: Interfacial Capacitances and Sulfur Coverage of Clean and Modified Au and Pd Electrodes

	capacitance[c]		sulfur coverage (θ_S)	
	Au	Pd	Au	Pd
clean	26 ± 5	123 ± 8		
S modified	21 ± 3	26 ± 3	from 1/3 to 2/3[a]	0.8 ± 0.1
C3 covered	6 ± 1	10 ± 2	0.33[b]	0.78 ± 0.09
C12 covered	2.5 ± 0.8	4.5 ± 1.4	0.33[b]	0.76 ± 0.09

[a] Estimated according with refs 45 and 46. [b] Data taken from refs 34 and 35. [c] μF·cm^{-2}.

potential at 50 mV·s^{-1} between −0.40 and −0.60 V, where interfacial capacitance is practically constant,[44] and in a potential region which is near the potential of zero charge of Pd in basic electrolyte.[29] For the sake of comparison, we have also performed capacitance measurements on clean and alkanethiolate covered preferred oriented Au(111) substrates (Table 2). Table 2 also includes capacitance data for S modified Au and Pd electrodes.

As already reported for Au,[42,47] it is evident that both C3 and C12 adlayers significantly reduce the Pd capacitance (Table 2). We have also observed for these adlayers on Pd the well-known dependence of the capacitance value on the chain length: it is markedly smaller in C12 than in C3 adlayers. However, capacitances for shorter chain lengths are sometimes greater than those expected for a perfect blocking layer. The increased capacitance is indicative of partial permeation of electrolyte ions into the shorter adsorbed thiolates. In other words, the observed capacitance values for short chain thiolates could be greater than those expected for a perfect dielectric layer, due to the presence of pinholes and defects. In fact, short-chain alkanethiolate monolayers contain different types of defects such as missing rows[48] and molecular defects, where the molecules are absent or disordered, and domain boundaries, where the adsorbed alkanethiolates exhibit strong disorder.[49]

Since the decrease in the capacitance is related with a low dielectric constant layer on the electrode surface, it is clear that the low capacitances values obtained for alkanethiol modified Pd substrates should be ascribed to the presence of the hydrocarbon chains. However, in contrast to that observed for alkanethiolate SAMs on Au or Ag,[22−24] no reductive desorption peak was observed in the negative scans shown in Figure 3 in agreement with previously reported data.[21] Therefore, we studied the electrodesorption process combining the interfacial capacitance measurements and XPS after polarizing SAM modified Pd electrodes at different negative potentials.

3.4. Reductive Desorption of Alkanethiolate−Sulfide Adlayers. In order to study the electrodesorption process, capacitance data were recorded after (i) scanning the potential from −0.40 V to different negative potential limits (E_c) at 50 mV·s^{-1}, (ii) polarizing for 30 s at E_c, and (iii) scanning the potential between −0.40 and −0.60 V until reaching a stationary voltammogram. In these experiments, E_c was changed progressively in the negative direction. It is clear from the inset in Figure 4a that in the −0.60/−1.20 V potential range the double layer charging current remains low, i.e., the Pd surface remains blocked, but when E_c is < −1.20 V a progressive increase in the double layer current is observed, suggesting that the thiolate are desorbed from the surface.

The capacitance increase can be correlated with a decrease in the coverage by organic species. Then, the remaining coverage, θ_{rem}, can be directly estimated from the capacitance measurements.[41,50] As the maximum thiolate coverage could not be the same for the different thiols, θ_{rem} should be seen as a normalization quantity instead of a real coverage. Furthermore, some differences should be expected between θ_{rem} and the coverages obtained from XPS data. In Figure 4a we have plotted θ_{rem} vs E_c for C3 covered Pd electrodes. Similar results have been obtained for C6, C9, and C12 modified Pd substrates (see the Supporting Information). For C3 modified surfaces, desorption starts at a slightly more positive potential than for the C12 ones. This is reasonable, considering that for shorter chain alkanethiols weaker chain−chain interactions are expected. However, the observed difference (≈0.08 V), which is within the experimental error, is smaller than that reported for the same thiols on Au(111): 0.3 V.[23,24] In order to compare the capacitance and XPS data we have included in Figure 4a the θ_S values estimated from the XPS data for C3 at the different E_c values. It can be seen that the XPS information is in reasonable agreement with the capacitance data. In fact, at $E_c = -1.2$ V θ_S is the same than that measured for the as-prepared SAMs. On the other hand, at $E_c = -1.7$ V almost all the S species was desorbed. It was also found that the residual amount of S is larger for C12 than for C3, possibly because of the smaller solubility of the oxidized thiol species that remains physisorbed on the Pd surface (see the Supporting Information).

The desorption of the complex thiolate−sulfide adlayer was followed in detail by XPS experiments. Spectra taken for a

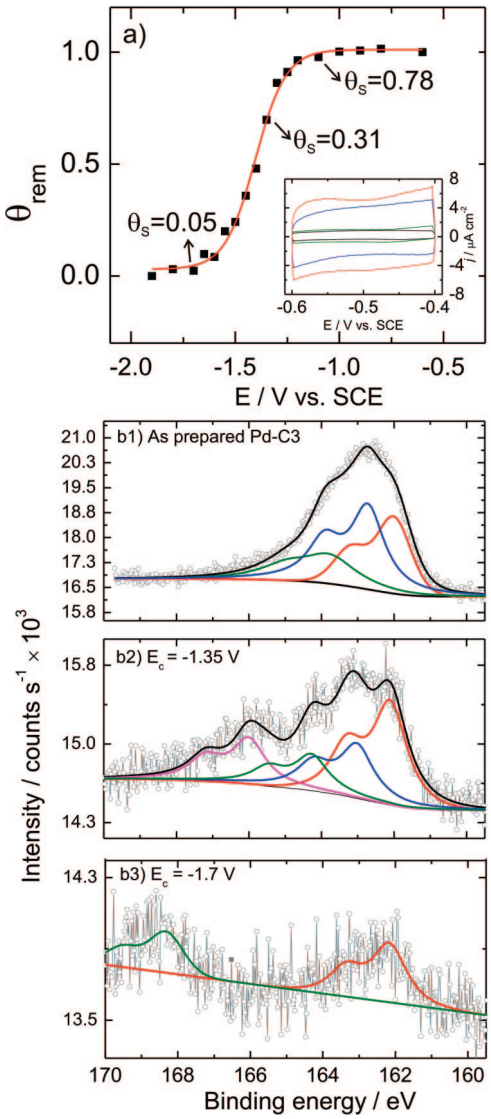

Figure 4. (a) Alkanethiol coverage, θ_{rem}, vs E_c for C3 modified Pd electrodes. θ_S obtained from XPS data at different potentials are also indicated. Inset: cyclic voltammograms recorded in NaOH 0.1 M for the measurement of electrode capacitances. Scan rate: 50 mV·s^{-1}. Black trace: as-prepared; green trace: $E_c = -1.2$ V; blue trace: $E_c = -1.4$ V; red trace: $E_c = -1.7$ V. (b) XPS spectra of a C3 modified Pd electrode. (b1) pristine, (b2) after polarization at $E_c = -1.35$ V, and (b3) after polarization at $E_c = -1.70$ V.

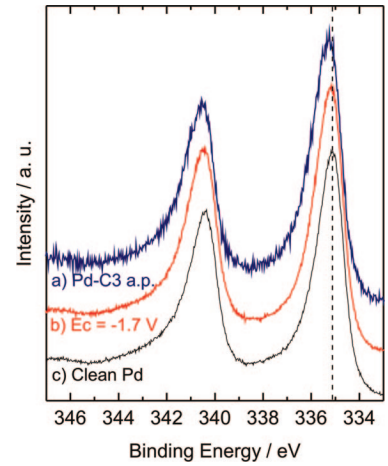

Figure 5. Pd 3d region XPS spectra of (a) an as-prepared C3 SAM on Pd, (b) after polarizing the sample at $E_c = -1.7$ V, and (c) clean Pd (for comparison, see also Figures 1 and 2).

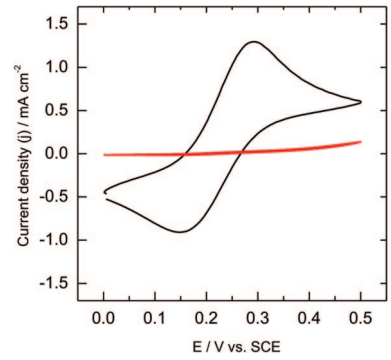

Figure 6. Voltammograms of C12 modified Pd electrode in 10 mM $K_4Fe(CN)_6$ solution in 1 M KNO_3. Scan rate: 100 mV·s^{-1}. Red trace: as-prepared C12 SAM, black-trace: after reductive desorption.

pristine adlayer prepared from C3 and those taken after applying different negative potentials (E_c) are shown in Figure. 4b1, b2, and b3, respectively. The analysis of these spectra reveals a marked decrease in the θ_S from approximately 0.8 to 0.05 as E_c moves negatively, as expected for the reductive desorption of sulfur-containing species. We observed some preferential desorption of the thiolate component (162.9 eV) at first. In Figure 4b, the signal assigned to the thiolate component is shifted toward higher BE as the coverage decreases. This could be attributed to the fact that the surface changes from a complex thiolate-sulfide adlayer to a Pd surface which is almost free of sulfur. Simultaneously, the formation of oxidized species at 166−168 eV along the reductive desorption process was observed. This suggests that the process of thiolate electrodesorption from Pd might progress in different steps. Nevertheless a more detailed study of this process should be done in order to elucidate the precise mechanism of the adlayer desorption from Pd. It is also evident that the residual amount of S (θ_S = 0.05) consists mainly of sulfide and oxidized S species (Figure. 4b3). It has been reported that monomeric S strongly chemisorbed at step edges remains adsorbed after S electrodesorption from Au(111) terraces.[35] We have also studied the Pd 3d region in order to decide whether the Pd surface recovers its metallic state after adlayer desorption. Figure 5 shows XPS spectra taken for a pristine C3 modified substrate (Figure 5a), this sample polarized at $E_c = -1.7$ V (Figure 5b) and for a fresh Pd sample after electrodeposition (Figure 5c). It is clear that after the reductive desorption the Pd 3d XPS signal shows that Pd has almost recovered the metallic character (Figure 5b). The fact that the Pd 3d signal is not exactly located at the same BE of 3d electrons in clean Pd could be ascribed to the few amount of residual S at $E_c = -1.7$ V.

3.5. Charge Transfer through the Thiolate−Sulfide Adlayer. In order to further test the charge transfer blockage introduced by the complex adlayer we have measured the electrochemical response of a redox couple in solution which does not penetrate alkanethiol SAMs.[51,52] We measured the ferro/ferricyanide redox couple voltammetric response both in the as-prepared C12 adlayer and after the completion of the reductive desorption experiment. The cyclic voltammetry was done in an electrochemical cell containing a 10 mM $K_4Fe(CN)_6$ solution in 1 M KNO_3. The voltammograms obtained are shown in Figure 6. The pristine adlayer formed from C12 has a blocking effect to the charge transfer. Only a small positive current which increases quasiexponentially with the overpotential is observed. It is also interesting to note that no plateau or peak currents, which could be related to mass transfer limited

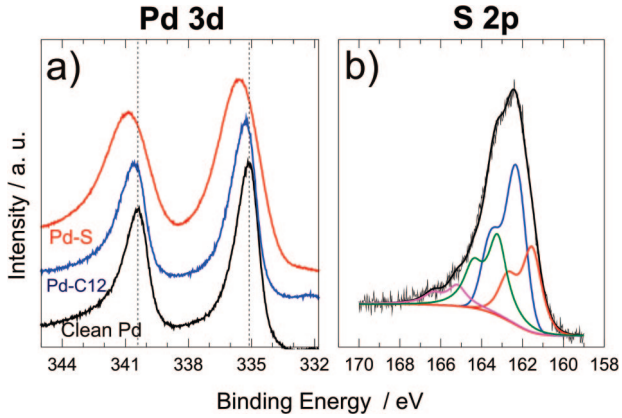

Figure 7. (a) Comparison of Pd 3d XPS signals of Pd electrodes, clean and modified with S or C12. (b) S 2p signal of Pd modified with S.

processes, are seen. Then, we speculate that the low positive signal registered mainly corresponds to tunneling current through the adlayer.[42] This clearly demonstrates that a dense alkanethiolate-containing adlayer is formed on Pd, similar to C12 SAM on Au.[49,51] After thiolate reductive desorption, the typical redox couple behavior was reached, which shows that an alkanethiol free Pd electrode was obtained, as expected by the previous results.

It was pointed out by Soreta et al. that some problems could be encountered in the electrochemical characterization of SAMs on Pd using the ferro/ferricyanide redox couple because of the Pd dissolution on the anodic region.[9] However the Pd oxidation would not interfere in the case of the complete C12 monolayer because the electrolyte has negligible access to the Pd surface.

3.6. Sulfur Adsorption on Pd. The fact that the potential of reductive desorption of alkanethiols on Pd does not change significantly with the hydrocarbon chain length suggests that the complex nature of the adlayer structure, in particular the presence of metallic sulfide, plays a key role in stabilizing the adlayer. Therefore, we have prepared S-modified surfaces by immersing Pd substrates in a diluted Na_2S aqueous solution for a short time. The XPS data for the Pd 3d and S 2p signals shown in Figure 7a-b are consistent with the formation of a S adlayer on Pd. The shift of Pd 3d signal to higher BEs in S covered Pd is approximately 0.5 eV, as described before.[53] This shift is larger than the one encountered in C12 covered Pd (Figure 7a). The presence of the 161.6 and 162.4 eV components suggests the existence of PdS and PdS_2 respectively, while the component at 163.3 eV can be assigned to S_n species[53] (Figure 7b). A small amount of oxidized S is also present as revealed by the signal at 165.2 eV.

The electrochemical behavior of this sulfur layer was studied in conditions similar to those previously described for alkanethiols. In Figure 8 a typical voltammogram of Pd modified with approximately one monolayer of sulfur in 0.1 M NaOH is shown. It can be seen that the H adsorption reaction (peak CII in Figure 1b) is blocked and also the current density of PdO reduction (peak CI in Figure 1b) is lower than in clean Pd, as expected for sulfur poisoned electrodes.[54] An extra anodic peak (AIV) is observed in the potential region of PdO formation. This peak is due to the oxidative desorption of the chemisorbed S species.[54,55]

The most important sulfur species present in NaOH 0.1 M aqueous solution is SH^-. Therefore, the process of S adsorption can be written as

$$Pd + HS^- + OH^- \rightarrow PdS_{ads} + 2e + H_2O$$

The reductive desorption reaction is the inverse to the adsorption reaction.

The fact that H adsorption process is blocked in the electrode modified with sulfur was used as an electrochemical probe to study the reductive desorption of sulfur from Pd. A sulfur-modified Pd electrode was polarized at different negative potentials (E_c) for 1 min and then the H adsorption reaction was studied by cyclic voltammetry between −0.40 V and −1.00 V. In Figure 9 the volammograms obtained after polarizing a S-modified sample at different E_c are shown. It can be seen that after polarization at −1.30 V the H adsorption (peak CII in Figure 1 and 8) reaction remains blocked. Only after polarizing at −1.35 V does the H adsorption peak appear, suggesting that S desorption starts in that potential region.

S coverage was also monitored by XPS (Figure 10). The coverage was calculated weighting principal components of S 2p regions since there are components of higher BE belonging to free material which do not strongly interact directly with the Pd substrate. It can be seen that at −1.20 V S desorption starts, and at −1.7 V the electrode is almost sulfur-clean. The fact that the substrate surface is practically S-clean at this potential value is also reflected in the 3d Pd level that shows the typical signal of metallic Pd (Figure 7a). The differences between XPS and electrochemical responses can be ascribed to the fact that little differences in coverage may not be noticeable by electrochemical measurements. However, these data indicate that S on Pd is electrodesorbed in the same potential region than alkanethiolates on Pd. This result suggests that the electrochemical behavior of alkanethiols on Pd is mostly leaded by sulfur and not by the hydrocarbon chains as observed in SAMs on other metals. This mechanism is consistent with the observed behavior of alkanethiolates on Pd, whose potentials of reductive desorption only slightly depend on the hydrocarbon chain length.

4. Conclusions

Our results from electrochemical techniques and XPS data confirm the presence of a complex adlayer on Pd consisting of thiolates and sulfides. From $\theta_S \approx 0.8$ and the relative intensity of the different S 2p components, the surface coverages by sulfide and thiolate result in $\theta_{Sulfide} \approx 0.4$ and $\theta_{thiolate} \approx 0.3$. The value $\theta_{thiolate} \approx 0.3$ is close to that found for thiolate SAMs on Au ($\theta_{thiolate} \approx 0.33$), explaining the barrier properties found in the electrochemical measurements. The value $\theta_{Sulfide} \approx 0.4$ is consistent with the formation of diluted palladium sulfide

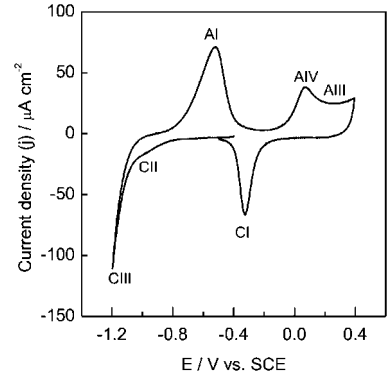

Figure 8. Voltammogram of Pd electrode incubated one minute in 60 μM Na_2S + 0.1 M NaOH solution. Scan rate: 100 mV s^{-1}. Base electrolyte: NaOH 0.1 M.

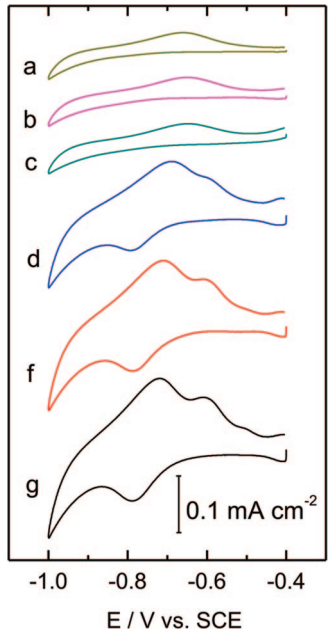

Figure 9. Voltammograms of a Pd electrode incubated 1 min in 60 microM Na_2S + 0.1 M NaOH and then polarized for 1 min at different potentials (E_c). (a) As-prepared, $E_c = -1.20$ (b), -1.30 (c), -1.35 (d), -1.40 (e), and -1.50 V (f). Scan rate: 100 mV·s^{-1}. Base electrolyte: NaOH 0.1 M.

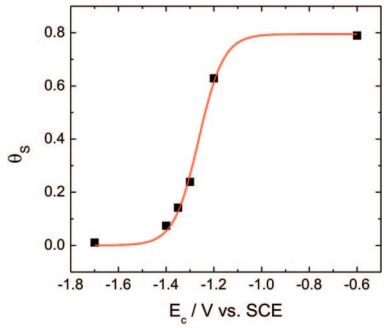

Figure 10. Sulfur coverage calculated from XPS measurements of the Pd electrode incubated for 1 min in 60 μM Na_2S + 0.1 M NaOH and then polarized for 1 min at different potentials (E_c).

layers.[7] The presence of some oxidation of Pd revealed by the XPS 3d spectra (not observed for Au) should be explained by the diluted sulfide layer close to the metal surface.[53] The complex sulfide-thiolate adlayer remains stable in a wide potential range. In fact, in contrast to previous findings for alkanethiolates on Pd in methanolic solutions,[21] the reductive desorption in aqueous 0.1 M NaOH takes place at $\approx$ 0.6 V more negative potentials than those observed for self-assembled monolayer of short thiols on Au,[56] while in the cases of Ag[23,57] and Ni[58] this difference is approximately 0.3 V (Figure 11). These differences become smaller for longer thiolate species due to the slight dependence of the reductive desorption on the hydrocarbon chain length observed for Pd.

The palladium sulfide layer can play a relevant role in stabilizing the complex adlayer in aqueous alkaline solutions explaining the smaller chain length dependence of the reductive desorption process. The fact that almost complete removal of the sulfide-thiol adlayer can be obtained by electrochemical methods is interesting because it opens a simple way to prepare carbon supported Pd nanoparticles (PdNPs) from thiolate-capped nanoparticles. It can be done by adsorption of thiolate-capped PdNPs on carbon substrates in hexane solution followed by

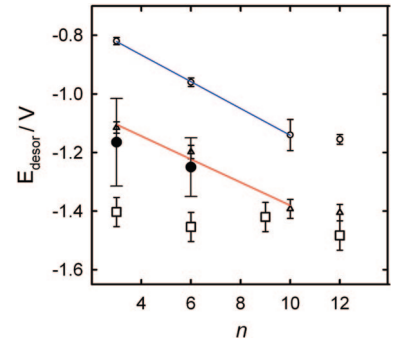

Figure 11. Reductive desorption potentials for alkanethiols of different chain length on different metals. (○ and blue trace) Au, (Δ and red trace) Ag, (●) Ni, (□) Pd.

simple and fast electrochemical cleaning of the S compounds in aqueous solutions, as reported for thiolate-capped Au nanoparticles.[59] On the other hand, the wide stability range of the thiolate-sulfide adlayers on Pd indicates that Pd could be a suitable platform for the fabrication of thiol-based sensors and biosensor devices in aqueous environments.

Acknowledgment. Financial support has been provided by the Argentine "Agencia Nacional de Promoción Científica y Tecnológica" (PICT 32980, PICT 0621, PICT 22711), CONICET and the National University of La Plata (Argentina). G.C. is a doctoral fellow of CONICET. R.C.S. is a Guggenheim Foundation Fellow. The authors thankfully acknowledge fruitful discussions with Francisco J. Ibañez.

Supporting Information Available: The results of the preparation (electrochemistry) and characterization (STM, XRD) of Pd substrates are presented. Also some details of the capacitance measurements and the results for C6, C9, and C12 are included. This material is available free of charge via the Internet at http://pubs.acs.org.

References and Notes

(1) Love, J. C.; Estroff, L. A.; Kriebel, J. K.; Nuzzo, R. G.; Whitesides, G. M. *Chem. Rev.* **2005**, *105*, 1103.
(2) Gates, B. D.; Xu, Q.; Stewart, M.; Ryan, D.; Willson, C. G.; Whitesides, G. M. *Chem. Rev.* **2005**, *105*, 1171.
(3) Ulman, A. *Chem. Rev.* **1996**, *96*, 1533.
(4) Azzaroni, O.; Vela, M. E.; Fonticelli, M.; Benitez, G.; Carro, P.; Blum, B.; Salvarezza, R. C. *J. Phys. Chem. B* **2003**, *107*, 13446.
(5) Schreiber, F. *J. Phys.: Condens. Mat.* **2004**, *16*, R881.
(6) Ferral, A.; Patrito, E. M.; Paredes-Olivera, P. *J. Phys. Chem. B* **2006**, *110*, 17050.
(7) Love, J. C.; Wolfe, D. B.; Haasch, R.; Chabinyc, M. L.; Paul, K. E.; Whitesides, G. M.; Nuzzo, R. G. *J. Am. Chem. Soc.* **2003**, *125*, 2597.
(8) Petrovykh, D. Y.; Kimura-Suda, H.; Opdahl, A.; Richter, L. J.; Tarlov, M. J.; Whitman, L. J. *Langmuir* **2006**, *22*, 2578.
(9) Soreta, T. R.; Strutwolf, J.; O'Sullivan, C. K. *Langmuir* **2007**, *23*, 10823.
(10) Williams, J. A.; Gorman, C. B. *Langmuir* **2007**, *23*, 3103.
(11) Carvalho, A.; Geissler, M.; Schmid, H.; Michel, B.; Delamarche, E. *Langmuir* **2002**, *18*, 2406.
(12) Love, J. C.; Wolfe, D. B.; Chabinyc, M. L.; Paul, K. E.; Whitesides, G. M. *J. Am. Chem. Soc.* **2002**, *124*, 1576.
(13) Zamborini, F. P.; Gross, S. M.; Murray, R. W. *Langmuir* **2001**, *17*, 481.
(14) Murayama, H.; Ichikuni, N.; Negishi, Y.; Nagata, T.; Tsukuda, T. *Chem. Phys. Let.* **2003**, *376*, 26.
(15) Sun, Y.; Frenkel, A. I.; Isseroff, R.; Shonbrun, C.; Forman, M.; Shin, K.; Koga, T.; White, H.; Zhang, L.; Zhu, Y.; Rafailovich, M. H.; Sokolov, J. C. *Langmuir* **2006**, *22*, 807.
(16) Ramallo-López, J. M.; Giovanetti, L.; Craievich, A. F.; Vicentin, F. C.; Marín-Almazo, M.; José-Yacaman, M.; Requejo, F. G. *Phys. B* **2007**, *389*, 150.
(17) Ibanez, F. J.; Zamborini, F. P. *Langmuir* **2006**, *22*, 9789.

(18) Berezin, M. Y.; Wan, K.-T.; Friedman, R. M.; Orth, R. G.; Raman, S. N.; Ho, S. V.; Ebner, J. R. *J. Mol. Catal. A: Chem.* **2000**, *158*, 567.
(19) Williams, J. A. *Ph.D. Thesis*, North Carolina State University, NC, 2004.
(20) Majumder, C. *Langmuir* **2008**, *24*, 10838.
(21) Williams, J. A.; Gorman, C. B. *J. Phys. Chem. C* **2007**, *111*, 12804.
(22) Kakiuchi, T.; Usui, H.; Hobara, D.; Yamamoto, M. *Langmuir* **2002**, *18*, 5231.
(23) Azzaroni, O.; Vela, M. E.; Andreasen, G.; Carro, P.; Salvarezza, R. C. *J. Phys. Chem. B* **2002**, *106*, 12267.
(24) Fonticelli, M.; Azzaroni, O.; Benitez, G.; Martins, M. E.; Carro, P.; Salvarezza, R. C. *J. Phys. Chem. B* **2004**, *108*, 1898.
(25) Martin, H.; Vericat, C.; Andreasen, G.; Hernandez Creus, A.; Vela, M. E.; Salvarezza, R. C. *Langmuir* **2001**, *17*, 2334.
(26) Kibler, L. A.; Kleinert, M.; Randler, R.; Kolb, D. M. *Surf. Sci.* **1999**, *443*, 19.
(27) Baldauf, M.; Kolb, D. M. *Electrochim. Acta* **1993**, *38*, 2145.
(28) Trasatti, S.; Petrii, O. A. *Pure Appl. Chem.* **1991**, *63*, 711.
(29) Grdeń, M.; Lukaszewski, M.; Jerkiewicz, G.; Czerwinski, A. *Electrochim. Acta* **2008**, *53*, 7583.
(30) Martin, M. H.; Lasia, A. *Electrochim. Acta* **2008**, *53*, 6317.
(31) Bolzán, A. E. *J. Electroanal. Chem.* **1995**, *380*, 127.
(32) Rieley, H.; Kendall, G. K.; Jones, R. G.; Woodruff, D. P. *Langmuir* **1999**, *15*, 8856.
(33) Yu, M.; Driver, S. M.; Woodruff, D. P. *Langmuir* **2005**, *21*, 7285.
(34) Vericat, C.; Vela, M. E.; Salvarezza, R. C. *Phys. Chem. Chem. Phys.* **2005**, *7*, 3258.
(35) Vericat, C.; Vela, M. E.; Benitez, G. A.; Gago, J. A. M.; Torrelles, X.; Salvarezza, R. C. *J. Phys.: Condens. Matter* **2006**, *18*, R867.
(36) Alfonso, D. R. *Surf. Sci.* **2007**, *601*, 4899.
(37) Zhong, C.-J.; Brush, R. C.; Anderegg, J.; Porter, M. D. *Langmuir* **1999**, *15*, 518.
(38) Vericat, C.; Vela, M. E.; Andreasen, G.; Salvarezza, R. C.; Vazquez, L.; Martin-Gago, J. A. *Langmuir* **2001**, *17*, 4919.
(39) Laredo, T.; Leitch, J.; Chen, M.; Burgess, I. J.; Dutcher, J. R.; Lipkowski, J. *Langmuir* **2007**, *23*, 6205.
(40) Bard, A. J.; Faulkner, L. R. *Electrochemical methods. Fundamentals and applications*, 2nd ed; John Wiley & Sons, Inc: New York, 2001.
(41) Damaskin, B. B.; Petrii, O. A.; Batrakov, V. V. *Adsorption of Organic Compounds on Electrodes*; Plenum Press: New York, 1971.
(42) Finklea, H. O. In *Electroanalytical Chemistry*; Bard, A. J., Rubinstein, I., Eds. Marcel Dekker: New York, 1996; Vol. 19, p 109.
(43) Torrelles, X.; Vericat, C.; Vela, M. E.; Fonticelli, M. H.; DazaMillone, M. A.; Felici, R.; Lee, T. L.; Zegenhagen, J.; Munoz, G.; Martin-Gago, J. A.; Salvarezza, R. C. *J. Phys. Chem. B* **2006**, *110*, 5586.
(44) Grdeń, M. *Electrochim. Acta* **2009**, *54*, 909.
(45) Vericat, C.; Andreasen, G.; Vela, M. E.; Salvarezza, R. C. *J. Phys. Chem. B* **2000**, *104*, 302.
(46) Lustemberg, P. G.; Vericat, C.; Benitez, G. A.; Vela, M. E.; Tognalli, N.; Fainstein, A.; Martiarena, M. L.; Salvarezza, R. C. *J. Phys. Chem. C* **2008**, *112*, 11394.
(47) Widrig, C. A.; Chung, C.; Porter, M. D. *J. Electroanal. Chem.* **1991**, *310*, 335.
(48) Hagenstrom, H.; Schneeweiss, M. A.; Kolb, D. M. *Langmuir* **1999**, *15*, 2435.
(49) Benitez, G.; Vericat, C.; Tanco, S.; Remes Lenicov, F.; Castez, M. F.; Vela, M. E.; Salvarezza, R. C. *Langmuir* **2004**, *20*, 5030.
(50) Lemay, D. M.; Shepherd, J. L. *Electrochim. Acta* **2008**, *54*, 388.
(51) Sabatani, E.; Rubinstein, I. *J. Phys. Chem.* **1987**, *91*, 6663.
(52) Flynn, N. T.; Tran, T. N. T.; Cima, M. J.; Langer, R. *Langmuir* **2003**, *19*, 10909.
(53) Rodriguez, J. A.; Chaturvedi, S.; Jirsak, T. *Chem. Phys. Lett.* **1998**, *296*, 421.
(54) Qian, S. Y.; Conway, B. E.; Jerkiewicz, G. *Int. J. Hydrogen Energy* **2000**, *25*, 539.
(55) Casella, I. G.; Guascito, M. R.; Desimoni, E. *Anal. Chim. Acta* **2000**, *409*, 30.
(56) Vela, M. E.; Martin, H.; Vericat, C.; Andreasen, G.; Hernandez Creus, A.; Salvarezza, R. C. *J. Phys. Chem B* **2000**, *104*, 11878.
(57) Hatchett, D. W.; Uibel, R. H.; Stevenson, K. J.; Harris, J. M.; White, H. S. *J. Am. Chem. Soc.* **1998**, *120*, 1062.
(58) Bengio, S.; Fonticelli, M.; Benitez, G.; Creus, A. H.; Carro, P.; Ascolani, H.; Zampieri, G.; Blum, B.; Salvarezza, R. C. *J. Phys. Chem. B* **2005**, *109*, 23450.
(59) Grumelli, D.; Vericat, C.; Benitez, G.; Vela, M. E.; Salvarezza, R. C.; Giovanetti, L. J.; Ramallo-Lopez, J. M.; Requejo, F. G.; Craievich, A. F.; Shon, Y. S. *J. Phys. Chem C* **2007**, *111*, 7179.

JP9001077